

Research



Cite this article: Pates S, Botting JP, McCobb LME, Muir LA. 2020 A miniature Ordovician hurdiid from Wales demonstrates the adaptability of Radiodonta. *R. Soc. Open Sci.* **7**: 200459. <http://dx.doi.org/10.1098/rsos.200459>

Received: 25 March 2020

Accepted: 18 May 2020

Subject Category:

Organismal and evolutionary biology

Subject Areas:

palaeontology

Keywords:

Afon Gam Biota, Dol-cyn-Afon Formation, Radiodonta, Hurdiidae, Ordovician, Lagerstätten

Author for correspondence:

Stephen Pates

e-mail: stephenpates@fas.harvard.edu

A miniature Ordovician hurdiid from Wales demonstrates the adaptability of Radiodonta


Stephen Pates¹, Joseph P. Botting^{2,3}, Lucy

M. E. McCobb² and Lucy A. Muir²

¹Museum of Comparative Zoology and Department of Organismic and Evolutionary Biology, Harvard University, Oxford Street, Boston, MA 02138, USA

²Department of Natural Sciences, Amgueddfa Cymru-National Museum Wales, Cathays Park, Cardiff CF10 3NP, UK

³Nanjing Institute of Geology and Palaeontology, Chinese Academy of Sciences, 39 East Beijing Road, Nanjing 210008, People's Republic of China

 SP, 0000-0001-8063-9469; LMEM, 0000-0002-8035-3337; LAM, 0000-0001-6324-2259

Originally considered as large, solely Cambrian apex predators, Radiodonta—a clade of stem-group euarthropods including *Anomalocaris*—now comprises a diverse group of predators, sediment sifters and filter feeders. These animals are only known from deposits preserving non-biomineralized material, with radiodonts often the first and/or only taxa known from such deposits. Despite the widespread and diverse nature of the group, only a handful of radiodonts are known from post-Cambrian deposits, and all originate from deposits or localities rich in other total-group euarthropods. In this contribution, we describe the first radiodont from the UK, an isolated hurdiid frontal appendage from the Tremadocian (Lower Ordovician) Dol-cyn-Afon Formation, Wales, UK. This finding is unusual in two major aspects: firstly, the appendage (1.8 mm in size) is less than half the size of the next smallest radiodont frontal appendage known, and probably belonged to an animal between 6 and 15 mm in length; secondly, it was discovered in the sponge-dominated Afon Gam Biota, one of only a handful of non-biomineralized total-group euarthropods known from this deposit. This Welsh hurdiid breaks new ground for Radiodonta in terms of both its small size and sponge-dominated habitat. This occurrence demonstrates the adaptability of the group in response to the partitioning of ecosystems and environments in the late Cambrian and Early Ordovician world.

1. Introduction

Lower Palaeozoic strata known for the exceptional preservation of lightly sclerotized or soft-bodied faunas (*Konservat-Lagerstätten*), deposited during the Cambrian and Early Ordovician (540–480 Ma), provide crucial information on the phylogenetic, morphological and ecological diversity patterns of early animals in marine environments (e.g. [1–4]). Radiodonts, a group which includes the large apex predator *Anomalocaris*, are among the best-known animals from these early ecosystems [5–13]. This diverse group of stem-group euarthropods (*sensu* [14]) is known from deposits ranging from China (e.g. [15–20]) to North America (e.g. [7,12,13,21–29]), Europe [25,30,31], North Africa [32,33] and Australia [34–36], reflecting the widespread nature of these (mostly) nektonic animals across different palaeocontinents from the equator to the poles.

On account of their lightly sclerotized frontal appendages, head sclerites and mouthparts, which sit anterior to a segmented body with lateral swimming flaps, radiodonts are often among the first animals described from *Konservat-Lagerstätten* (e.g. [8,32,37,38]). They are identifiable to the family, genus or even species level from their frontal feeding appendages alone (e.g. [24,25,29]). Members of the families Amplectobeluidae and Anomalocarididae possess appendages in which endites are alternately long and short on adjacent podomeres (e.g. [11,17]), in contrast with members of Tamisiocarididae and Hurdiidae, in which endites do not alternate in length (e.g. [26,27,31,35]). Tamisiocaridids differ from hurdiids in possessing paired slender endites along the entire appendage, whereas hurdiids have elongate endites (usually broad and recurved) on the five podomeres following the shaft region [24: fig. 1]. In addition, hurdiids sometimes have one to three podomeres with reduced endites distal to the five large-endite-bearing podomeres, and the distal podomeres reduce substantially in size compared with the tall rectangular podomeres in the proximal region [24,26–29].

Recent discoveries have shown that radiodonts occupied an array of ecological niches, from apex predators such as *Amplectobelua*, *Anomalocaris* and *Lyrarapax* [7,11,16–18,20] to sediment sifters such as *Cambroraster*, *Hurdia* and *Stanleycaris* [21,26–28], to the filter feeders *Aegirocassis*, *Pahvantia* and *Tamisiocaris* [31,33,39]. The Cambrian sites from which radiodonts have been reported all possess a rich co-occurring euarthropod fauna (e.g. [8,40–48]).

Here, we report a sub-centimetre-sized radiodont from the Early Ordovician (Tremadocian, *ca* 480 Ma) Afon Gam Biota of the Dol-cyn-Afon Formation, Wales, UK [49]. This is the first representative of this group of stem-group euarthropods from the UK, the first from the palaeocontinent Avalonia and the first from an environment dominated by sponges, rather than euarthropods. The small size of the specimen, which is less than half the size of the next smallest radiodont frontal appendage discovered, and the composition of the co-occurring fauna demonstrate the ecological adaptability of this important Palaeozoic group.

2. Material and methods

The radiodont is known from a single specimen, part and counterpart (NMW 2012.36G.90a,b) held at the National Museum Wales (NMW), Cardiff, Wales, UK, under accession NMW 2012.36G. This specimen was collected during fieldwork conducted in 2012, from a loose block in a small quarry at the foot of the Ceunant-y-garreg-ddu stream section (figure 1*a*).

Photographs were taken of the fossil both dry and wet, using a Leica Z6 microscope attached to a Canon 80D camera and stacked using Helicon Focus software.

Palaeogeography for the Tremadocian was reconstructed using GPlates 2.20 [50]. Figures and line drawings were created using Inkscape 0.92.

3. The Afon Gam Biota and comparable *Lagerstätten*

The Afon Gam Biota is located in North Wales (figure 1*a*). This deposit was part of the palaeocontinent Avalonia, which was separated from Gondwana towards the end of the Cambrian Period due to the opening of the Rheic Ocean [51]. During the Early Ordovician, Avalonia was located at mid to high latitude in the Southern Hemisphere. Different reconstructions place the continent around 60° latitude (e.g. [52–54]; figure 1*b*), or between 30 and 60° latitude (e.g. [55]).

In common with many other Palaeozoic marine *Konservat-Lagerstätten*, the Afon Gam Biota is rich in sponges. Unusually, trilobites are relatively scarce and other euarthropods are rare, especially when the

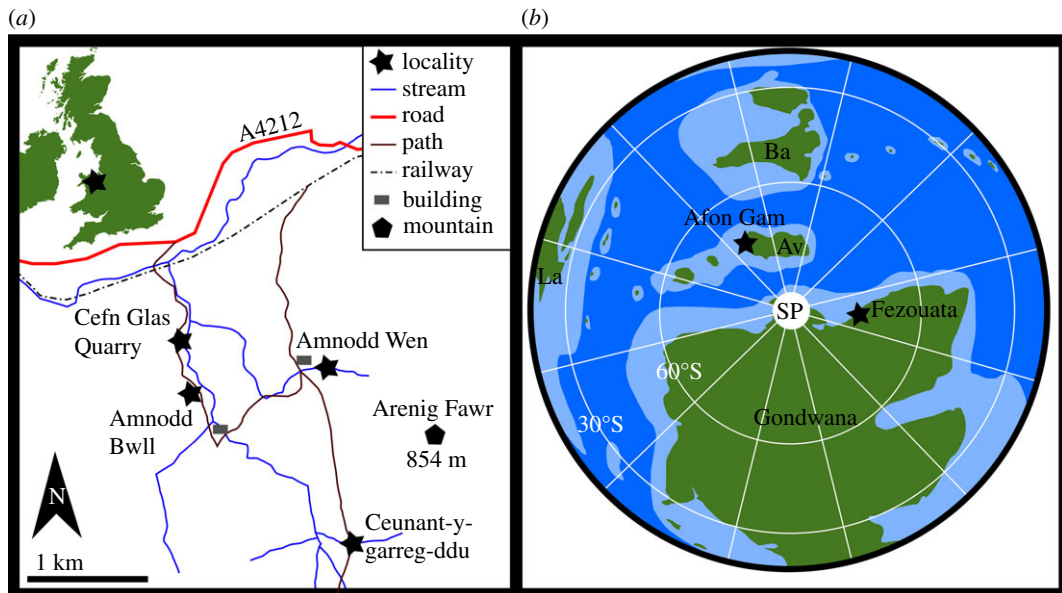


Figure 1. Geographical (a) and palaeogeographical (b) location of the Afon Gam Biota, Wales, UK. (a) Redrawn from [49]; (b) constructed using GPlates [50]. Av, Avalonia; Ba, Baltica; La, Laurentia; SP, South Pole.

potential for additional fossil material produced through the act of moulting is considered [49,56]. Given the diversity and preservation of other faunal elements, including sponges, worms and algae, the low density of euarthropods and their overall small size is probably not caused by taphonomic factors [49]. Sub-centimetre-sized bivalved euarthropod carapaces co-occur with rare, multi-centimetre fragments of larger euarthropods, and other taxa such as a several-centimetre priapulid worm, small palaeoscoleccids and large agglutinated tubes and sponges [49,57].

The Afon Gam assemblage may usefully be contrasted with the slightly younger Fezouata Biota of Morocco (e.g. [58–61]) and faunas described from Cambrian Burgess Shale-type (BST) deposits (e.g. [46,48]). The community of the Afon Gam Biota is known from a few localities over a relatively small area (figure 1; [49]); however, the community composition does not greatly vary among these sites [49]. The Afon Gam Biota represents a BST community in which euarthropods are a relatively minor part of the total assemblage [49]. By contrast, total-group euarthropods comprise between one-quarter and half of the biodiversity of Cambrian exceptionally preserved faunas (e.g. [45,48,62]). Sponge communities in Cambrian exceptionally preserved faunas are remarkably consistent both temporally and geographically [63], and across all phyla at the genus level, communities became globally more homogeneous across the Stage 4–Wuliuan boundary [46]. Similarly, the Ordovician Fezouata Biota as a whole contains a high diversity of euarthropods sampled from a large number of sites; however, many assemblages are low diversity and dominated by one or two taxa, and some taxa are known only from a handful of specimens at a single site [58,64].

Some younger Ordovician *Konservat-Lagerstätten* exhibit a sponge-dominated ecology superficially similar to the Afon Gam Biota, with a comparable rarity of non-trilobite euarthropods [65,66]. These communities are all faunally distinct from each other, consistent with the increasing community disparity of the Great Ordovician Biodiversification Event. At least among euarthropods, this increasing disparity was either linked with or subsequent to a global restructuring of communities in the late Cambrian marked by several extinction events (e.g. [43,67,68]).

4. Fossil description

4.1. Terminology and organization of hurdiid frontal appendages

The single specimen preserved as part and counterpart (NMW 2012.36G.90a, b; figures 2 and 3) probably represents an isolated frontal appendage of a new genus and species of hurdiid radiodont (§4.3). As a result, the description uses terminology associated with hurdiid radiodonts, although alternative taxonomic hypotheses for the specimen are also considered (§4.4).

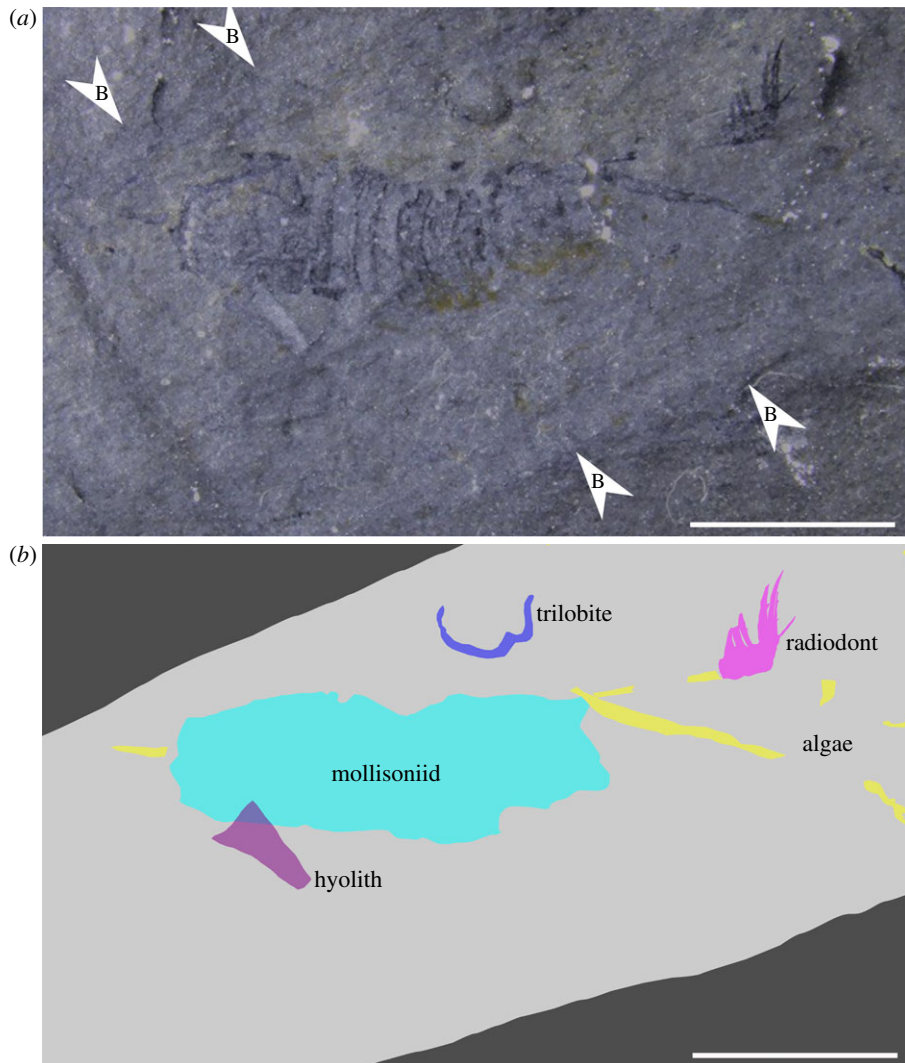


Figure 2. NMW 2012.36G.90a from the Afon Gam Biota, Dol-cyn-Afon Formation, Wales, UK. Accumulation of fossil material in burrow, including hurdiid radiodont frontal appendage. (a) Photograph of specimen, taken under water; (b) interpretative drawing. B, edge of burrow. Scale bars: 5 mm.

Radiodont frontal appendages are separated into a ‘shaft’ region, which is generally the poorest known part of the appendage as it is less sclerotized than the endite-bearing ‘distal articulated region’ which follows it [19]. The shaft region (green, figure 4a) sometimes bears an endite at its most distal point, though not in all cases (for example, the hurdiid *Peytoia nathorsti* lacks a shaft endite [7,24]).

In hurdiids, the distal articulated region can be separated into two further parts. The proximal five podomeres following the shaft bear elongate endites (grey, figure 4a), which are generally unpaired and broad rather than spiniform (a single exception is *Ursulinacaris grallae*, which bears paired slender endites [24]). Endites on these proximal five podomeres in the distal articulated region bear auxiliary spines (rarely setae [33,39]) on their distal margin only. Distal to these five podomeres is sometimes one to three podomeres bearing a reduced endite (blue region, figure 4a), although some hurdiids (e.g. *Aegirocassis benmoulaei* [33]) do not bear any reduced endites. Sometimes a podomere which does not bear an endite separates the reduced endite-bearing podomere from the five podomeres bearing large endites [26]. Hurdiid appendages terminate in a number of podomeres that do not bear endites, and at least one terminal spine (pink, figure 4a).

4.2. Secondary concentration of material within a burrow

The specimen NMW 2012.36G.90 is preserved close to the body of a mollisoniid-like animal. As non-trilobite euarthropods are rare in the Afon Gam Biota [49], it might be assumed that the appendage

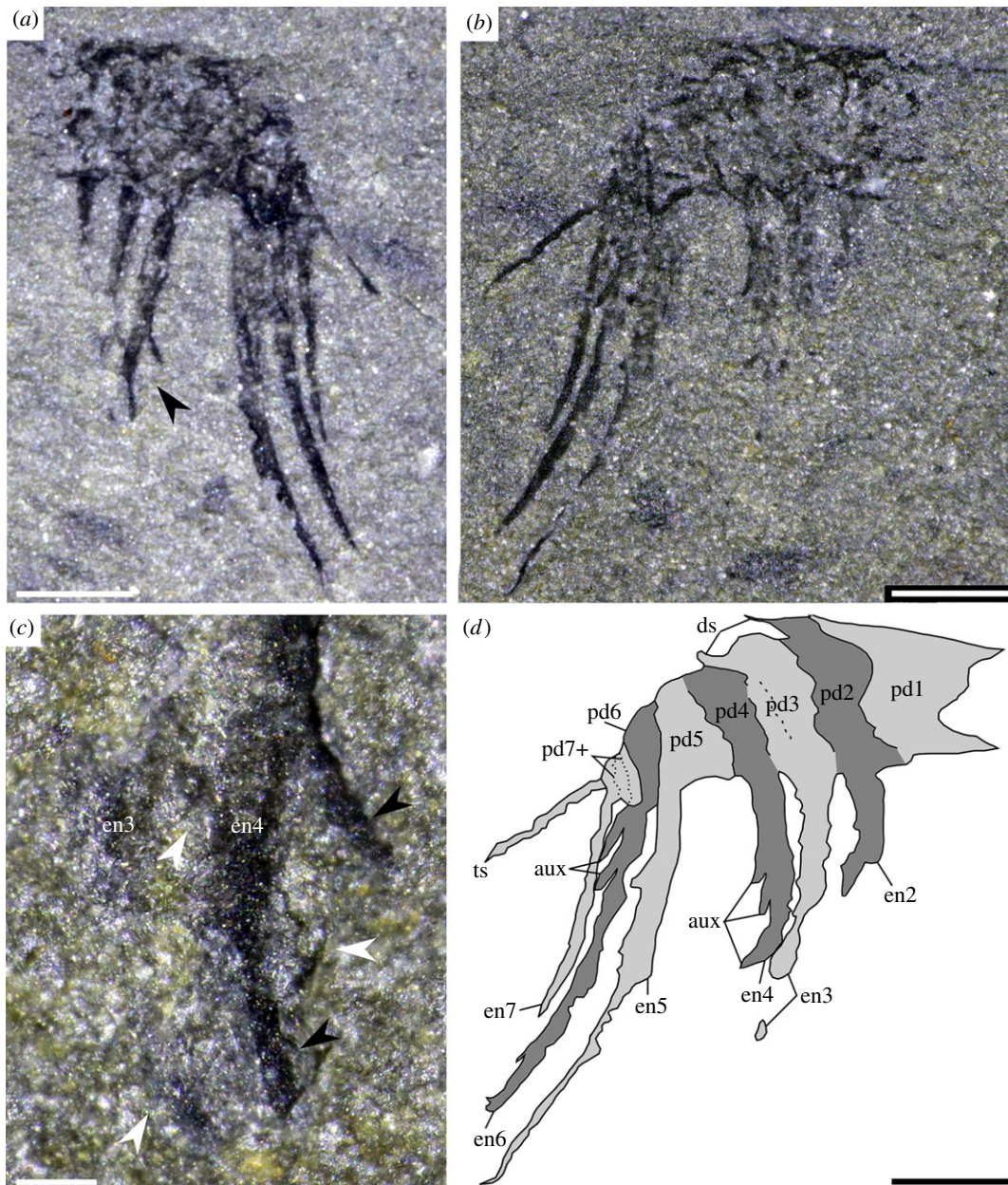


Figure 3. Close-up of hurdiid frontal appendage from figure 2. (a) Counterpart NMW 2012.36G.90b; (b) part NMW 2012.36G.90a; (c) area indicated by black arrow in (a), white arrows indicate auxiliary spines on endite 3, black arrows indicated auxiliary spines on endite 4; (d) interpretative drawing of the part. aux, auxiliary spines; ds, dorsal spines; en, endite; pd, podomere; ts, terminal spine. Scale bars: (a,b,d) 0.5 mm; (c) 0.1 mm.

belongs with that body. However, the mollisoniid-like animal and the appendage are inside a burrow, and co-occur with an adjacent hyolith conch, probable algal strands and trilobite fragments (figure 2). This assemblage indicates secondary concentration of the material, and so the two non-trilobite euarthropod specimens are considered to belong to different animals, as is implied by their morphology. It should also be noted that the close association of a hurdiid radiodont appendage with an unrelated body has previously been reported from Cambrian strata of the Holy Cross Mountains, Poland [30], although the context of that association (e.g. whether that material also was concentrated in a burrow) is unknown, as the material comes from a core section.

4.3. Description as a hurdiid radiodont frontal appendage

The isolated radiodont frontal appendage, preserved in lateral view, measures 1.8 mm along the dorsal margin from the proximal-most preserved part of the shaft region (figure 3, pd1) to the base of the

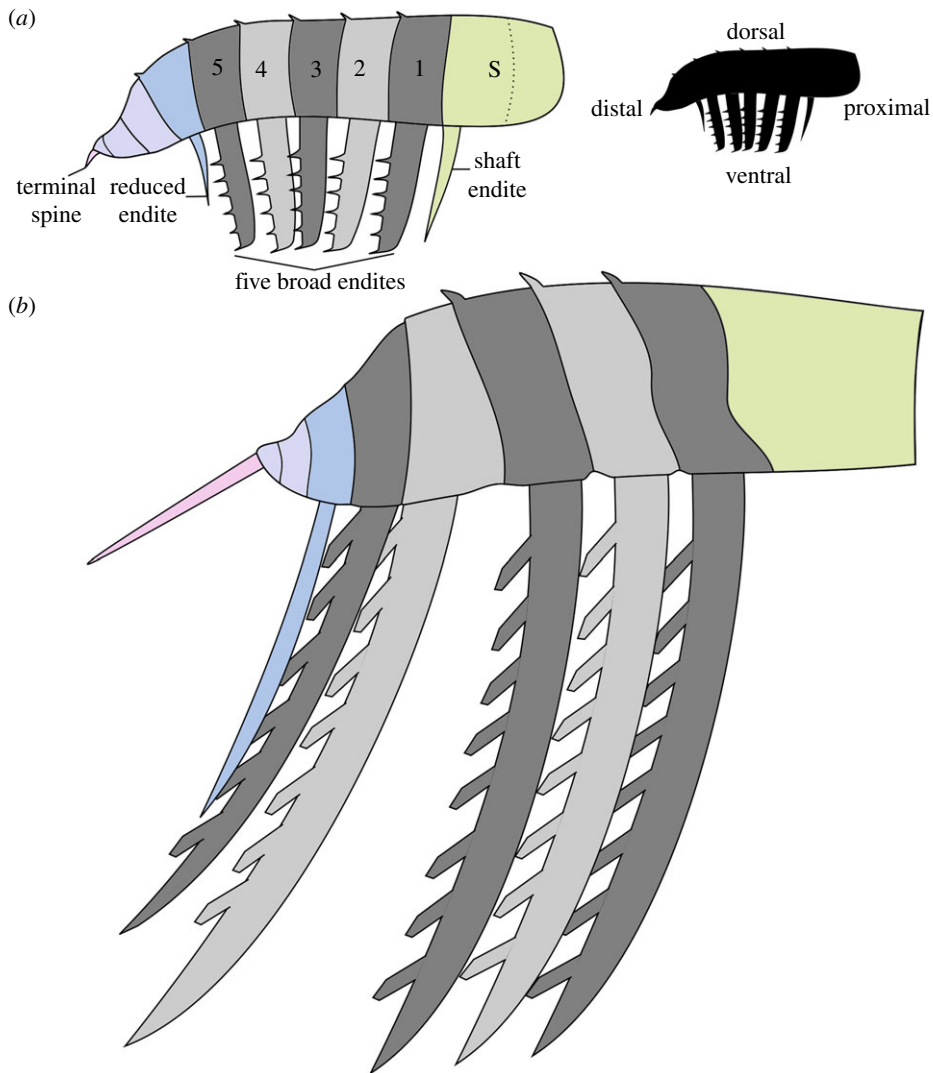


Figure 4. Comparison of an idealized hurdiid appendage and black silhouette illustrating terminology of distal, proximal, dorsal and ventral (a) with a reconstruction of the Afon Gam hurdiid (b). Colours indicate the proposed homologous parts of the appendage, as labelled in (a). 1–5, five podomeres bearing broad recurved endites; S, shaft region.

elongate and straight terminal spine (figure 3, ts), which measures 0.6 mm. Boundaries between six podomeres (figure 3, pd1–pd6) are clearly visible in the part (figure 3*b,d*). The preserved width of these podomeres, which represent the shaft (figure 3, pd1) and proximal five podomeres in the distal articulated region (pd2–pd6), is approximately 0.2 mm, with the measured heights reducing from 0.6 mm (figure 3, pd1–pd4) to 0.3 mm (figure 3, pd6). Distally, podomere boundaries are less discernible, but at least three, less than 0.15 mm in height, are visible in this area (figure 3, pd7+). Dorsal spines project from the distal margin of tall rectangular podomeres, most visible on pd2 and pd3 (figure 3, ds). Six blade-like endites are present on the appendage. No endite, either partial or complete, is visible on the shaft podomere. Three partial endites (figure 3, en2–en4) and two complete recurved endites (figure 3, en5 and en6) are present on the proximal five podomeres in the distal articulated region, and one complete but slightly shorter endite (1 mm length) is present distally (figure 3, en7). Complete endites are around four times the length of the podomeres to which they attach; for example, the longest, en5, measures 1.6 mm, and attaches to a podomere measuring 0.4 mm from ventral to dorsal margin. Incomplete partial endites (en2–en4) are expected to have reached similar lengths to the complete endites (en5 and en6) based on comparisons with other hurdiid frontal appendages, and their similar width at the preserved base (figures 4 and 5). Endites bear thin needle-like auxiliary spines which project at an angle between 130 and 160° to the distal margin of the endite to which they attach. Auxiliary spines measure 0.2 mm along their long axis, and are best preserved on the part of the endite closest to the podomere for en4–en6 (figure 3*c*, white and

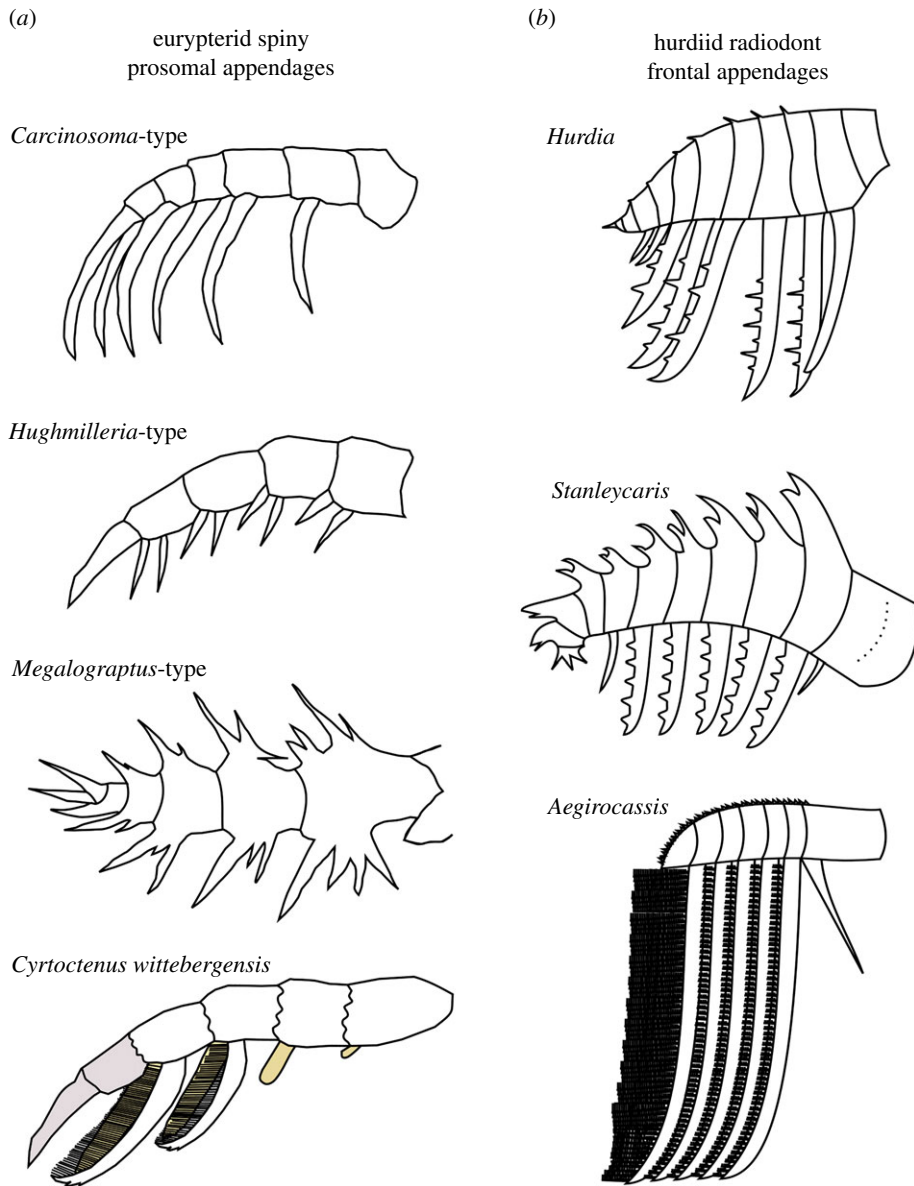


Figure 5. Comparison of distal regions of eurypterid spiny prosomal appendages (a) and hurdiid radiodont frontal appendages (b). Appendages orientated to provide best possible comparison with NMW 2012.36G.90. Reconstructions of *Carcinosoma*-type (taxa such as the Ordovician *Orcanopterus manitoulinensis*), *Hughmilleria*-type (taxa such as the Ordovician *Paraeurypterus anatolensis*) and *Megalograptus*-type (taxa such as the Ordovician *Pentecopecterus decorahensis*) eurypterid spiny appendages redrawn from [69: fig. 9]. Reproduced with permission. *Cyrtoctenus wittebergensis* reconstruction created using data from [70]. Note the finger-like movable spine visible (yellow) underneath the filamentous structures for *Cyrtoctenus wittebergensis*, and comparable structures on two podomeres which do not bear combs proximally. The distalmost two podomeres (seven and eight; brown) are not known in this species, and so reconstruction of this part is speculative.

black arrows; figure 3*d*, aux). The distance between the best preserved auxiliary spines (on en4; figure 3*a*, black arrow) is under 0.2 mm (measured between two spines indicated with black arrows in figure 3*c*). There is no evidence that the auxiliary spines were present along the whole length of the endites; indeed, the distal margin of the tipward region appears to be smooth for en5 and en6 (figure 3*a*). However, a comparison of the proximal region of en4, where the auxiliary spine closest to where the podomere meets the endite is only visible in the part not the counterpart (figure 3*b* not figure 3*a*), implies that auxiliary spines may have been present along most of the endite as seen in other hurdiids, and that the lack of auxiliary spines along most of the endites is preservational. It remains possible that spines are only found on the part of the endite closest to the podomere.

The presence of a blade-like endite on each of the proximal five podomeres in the distal articulated region, tall rectangular podomeres that reduce in height markedly in the distal portion and the presence

of auxiliary spines only on the distal margin of endites are all characters which support the identification of this specimen as the frontal appendage of a hurdiid radiodont. Under this hypothesis, the Welsh radiodont would lack a shaft endite, just as in the hurdiid *Peytoia nathorsti*, and the five proximal endites would be equivalent to the five blade-like endites known in all other hurdiids except for *U. grallae*, in which endites on these five podomeres are slender and paired [24] (grey podomeres and endites in figure 4). The distalmost endite (en7) would be equivalent to the reduced distal endites (blue endite in figure 4; ‘den’ in fig. 2 of [24]; ‘enditic spines’ of [26]) known in *Cambroraster*, *Hurdia*, *Stanleycaris*, *Ursulinacaris* and a taxon not yet formally described from the Burgess Shale (?*Laggania* of [29]), although such a comparatively long distal endite is only known in the latter two hurdiid radiodonts [21,23,24,26,27,29].

The orientation of the auxiliary spines (slightly oblique and pointing towards the tip of the endite, rather than perpendicular to the endite) is unique among hurdiids, but has been observed in the other three radiodont families: amplexobeluids (e.g. *Amplectobelua symbrachiata*; [10]); anomalocaridids (e.g. *Anomalocaris canadensis*; [11]); and tamisiocaridids (e.g. *Tamisiocaris borealis*; [31]). In each of these cases, auxiliary spines project from both the distal and proximal margins of endites. In all phylogenetic analyses which have attempted to shed light on the internal relationships of radiodonts, the sister group to hurdiids has been resolved as tamisiocaridids (‘Cetiocaridae’ of [31]; [15,20,31,33,39]) or in one case, amplexobeluids [26]. The presence of this character in a hurdiid is, therefore, less surprising, given its appearance in the sister group of the family, and in fact all other radiodont families. Indeed, given the phylogenetic frameworks of all these studies, the case observed in the Welsh radiodont can be considered to be the ancestral condition for Radiodonta, with the case in other hurdiids (a row of spines perpendicular to the endite) derived.

While the arrangement (five blade-like endites proximal to a reduced endite) and shape (recurved distally and broad) of endites is broadly similar to many hurdiids such as *Hurdia*, and *Stanleycaris* (figure 5) [21,27,28], the ca 4:1 ratio of endite length to podomere height in the Welsh hurdiid is only otherwise observed in the filter-feeding nektonic *Aegirocassis* (figure 5) and *Pahvantia*, and the eudemeral *Cambroraster* [26,33,39]. The orientation and spiniform nature of the auxiliary spines, the length and morphology of the terminal spine (a length that far exceeds that observed in other radiodonts, relative to the length of the appendage) and the relative length of the reduced distal endite provide a unique combination of characters that suggest that this specimen represents a new genus and species of hurdiid radiodont (reconstructed in figure 4b).

4.4. Alternative taxonomic hypotheses

Given the partial nature of the specimen, its small size, unusual depositional setting and novel characters—especially the length of the terminal spine—it is necessary to consider alternative taxonomic hypotheses. In two previous cases, material originally described as a lobopodian has been reidentified as a radiodont frontal appendage [23,25,71–73], and, given the small size of specimen NMW 2012.36G.90, such a hypothesis should be given some consideration. The lobopods of some lobopodians such as *Aysheaia pedunculata* from the Burgess Shale taper to a clawed tip. When preserved laterally compressed and curved towards the head end, these structures can give an overall blade-like appearance, similar to hurdiids [23: fig. 3D]. However, a lobopodian affinity for this specimen is discounted by the presence of boundaries (interpreted here as podomere boundaries) which cross the entire specimen and are more widely spaced than would be expected for the annulated body of a lobopodian.

The presence of podomere boundaries allows the identification of this specimen as a total-group euarthropod appendage. Eurypterids, crown-group euarthropods (Chelicerata) also known from the early Palaeozoic, possessed non-biom mineralized appendages, some of which bear a superficial resemblance to specimen NMW 2012.36G.90. Eurypterids bear six pairs of legs under the prosoma, which are referred to as appendages I–VI from anterior to posterior. Appendage I bore the chelicerae, while appendages II–V were walking legs with gnathobases, and sometimes spines [69,74]. In stylonurine eurypterids, appendages II–VI may differ slightly in size but all display broadly the same morphology, whereas in the other branch of the eurypterid tree, in eurypterines, appendages II and III have a raptorial function, appendages IV and V are walking legs and appendage VI is a specialized swimming paddle [69,74: fig. 26]. The spiniferous walking legs bear the most similarity to hurdiid radiodont frontal appendages. Eleven spiny walking leg morphologies were identified by Tollerton [69: fig. 9], and below we consider first morphologies known from the Ordovician, and then secondly a morphology known in derived freshwater eurypterids with recurved comb structures similar to the endites of hurdiid radiodont frontal appendages (figure 5).

The oldest known eurypterid, *Pentecopterus decorahensis*, was described from the Winneshiek Lagerstätte (Darriwilian; Iowa, USA [74]). This animal is younger than NMW 2012.36G.90, and so a eurypterid affinity for the Welsh animal would make it the oldest member of this group. *Pentecopterus* is a member of the family Megalograptidae, with other Ordovician eurypterids assigned to this family and Onychopterellidae, Orcanopteridae and Rhenopteridae [74–77]. A final Ordovician eurypterid, *Paraeurypterus anatolensis* from Turkey, has not been assigned to a family but belongs to the eurypterine branch (rather than the stylonurine branch) [78]. Of these groups, megalograptids possessed *Megalograptus*-type legs (figure 5) [69], onychopterellids and *P. anatolensis* bore *Hughmilleria*-type legs (figure 5) [69,75,78] and rhenopterids had unspiniferous legs [69]. Non-spiniferous, *Hughmilleria*-type and *Megalograptus*-type eurypterid walking legs share very few morphological characters with specimen NMW 2012.36G.90 beyond the presence of podomere boundaries, and spines in the latter two. The morphology of the spines, number per podomere and orientation, as well as position on the podomere, all differ from what is seen in the Welsh specimen, even when the leg is orientated to be as similar as possible (figure 5). For example, some elongate spines are known on some appendages of *P. decorahensis*; however, these are either straight or curve the opposite direction to the Afon Gam appendage, and are on the same podomeres as other spines [74: figs 3 and 10D]. Of the Ordovician eurypterids, the orcanopterid *Orcanopterus manitoulinensis* (Upper Ordovician; Manitoba, Canada) with its *Carcinosoma*-type legs (figure 5) [69,76] is most similar to the specimen described in this study. Although incomplete, the prosomal legs II–V of the Canadian eurypterid possess a single recurved spine from a single podomere; however, these spines curve in the opposite direction relative to the appendage than the endites in the Welsh animal (and hurdiid endites in general; figures 4a and 5) [76: figs 3.4 and 4.3], a character shared with other *Carcinosoma*-type appendages [69]. Distal podomeres in *O. manitoulinensis* bear only one spine, even on appendage V, where four podomeres can be observed [76: fig. 4.3]. This morphology contrasts with the multiple podomeres that bear endites in the Welsh animal, although it should be noted that other *Carcinosoma*-type appendages do preserve multiple podomeres bearing curved spines (figure 5). In addition to differences in the spine morphology in *Carcinosoma*-type appendages to the endites observed in the Welsh animal, the podomeres are also a different shape. In the Manitoban eurypterid, they are square to elongate rectangles, in contrast with the tall and thin rectangles in the Afon Gam appendage.

Disregarding temporal or environmental constraints, the comb-bearing appendages of the sweep-feeding eurypterid genus *Cyrtoctenus* (family Hibbertopteridae) share a number of morphological characters with the Afon Gam specimen, and hurdiid appendages in general [28,70,79]. This stylonurine family is known from Devonian and younger deposits, exclusively from freshwater environments, and has been considered a highly specialized and unusual group of eurypterids [80]. *Cyrtoctenus* appendages bear elongate recurved combs with numerous (more than 80) finely spaced filament structures extending from the concave margin (figure 5). The shape of the comb and margin bearing auxiliary structures is consistent with what can be observed in NMW 2012.36G.90; however, there are a number of significant morphological differences (figures 3–5). In *Cyrtoctenus*, each comb is associated with a movable finger-like spine (visible underneath filaments in figure 5) [70,81], of which there is no evidence in the Welsh specimen. In addition, although the appendages of *Cyrtoctenus* are not completely known, in the South African taxon *C. wittebergensis*, combs are present on at least two, and potentially up to four podomeres—combs are absent on the proximal four podomeres, present on podomeres five and six while podomeres seven and eight are not preserved [70]. Podomere seven could only have hosted a very small comb and it was almost certainly absent on the distalmost podomere eight, due to the physical constraints of hosting these combs on a walking leg [70]. In the type species, *C. peachi*, each comb and movable finger-like spine was originally described as a separate abdominal appendage, with five (appendages A through E) described altogether [79]. Comparing with what is known in *C. wittebergensis*, movable spines (appendages C, D and E) and one comb (appendage A) can be recognized in the type species, while appendage B can be interpreted either as a modified comb or movable spine [70]. Even assuming the maximum possible number of combs in *Cyrtoctenus* (four, extrapolated from the maximum number of movable fingers in *C. peachi* or the number of observed combs in *C. wittebergensis* plus the number of podomeres not preserved), an additional two are present in the Welsh animal. The combs differ in relative size in *Cyrtoctenus* and the Afon Gam animal. In *C. wittebergensis*, the distalmost comb on podomere six was probably longer than that of podomere five, as implied by the relative size of the accompanying movable finger [70], the opposite case to what is seen in NMW 2012.36G.90, in which the distalmost endite is reduced—a morphology also observed in other hurdiids, as mentioned above.

Thus, despite some morphological similarities between both lobopodian bodies and eurypterid spiny legs and the Welsh animal, including the presence of broad curved spines, some of which bear slender projections on the concave margin, many more characters support the interpretation of specimen NMW 2012.36G.90 as the isolated frontal appendage of a hurdiid radiodont. Of the two characters unknown in other hurdiid radiodonts—the elongate terminal spine and auxiliary spines orientated towards the tip of endites—the second is known in all other radiodont families and probably represents the plesiomorphic state for Radiodonta. The elongate terminal spine (relative to appendage length) is unknown in other members of the order, and could reflect ecological specialization. This character may also have changed during the growth of the animal, becoming shorter relative to appendage length; however, our current knowledge of radiodont development (discussed briefly below) does not support this hypothesis.

5. Discussion

5.1. A miniature Ordovician radiodont

The Afon Gam animal represents the smallest known hurdiid, and potentially radiodont, currently known. Literature data for appendage:body length ratios in complete radiodonts have previously been compiled (supplemental note in [39]). Extrapolating from these data and considering additional information from *Cambroraster* [26] and *Hurdia* [28], this animal was probably between 6 and 15 mm in length, although it could conceivably have been as small as *ca* 3.5 mm.

The extrapolated size range of 6–15 mm for this animal based on the size of the frontal appendages comes from comparisons with other hurdiid radiodonts. Complete specimens of the hurdiid *Peytoia nathorsti* from the Burgess Shale possess bodies between three-and-a-half and four times the length of their frontal appendages [7: figs 30 and 31; 39], giving the lower bound estimate for the likely length of this animal, 6 mm. Among radiodonts as a whole, complete specimens of *An. canadensis* can have frontal appendages approximately half the total length of the animal [11: figs 5 and 7; 39], which gives a possible, albeit unlikely, lowest bound estimate of *ca* 3.5 mm for the Welsh animal.

The relative length of appendages to body length is more difficult to determine in *Cambroraster* and *Hurdia*, due to the way that frontal appendages are often obscured by the carapace elements, and/or preserved incomplete and obliquely in complete or slightly disarticulated body specimens [26,28]. For *Hurdia*, a specimen in lateral view [28: fig. 21C,D] best shows the relationship between the length of the body and frontal appendages, as the carapace does not obscure the length of either; however, the proximal part of the appendage is overlain by the oral cone, preventing exact measurement. Taking only the visible portion, the frontal appendage in this specimen is approximately two-sevenths of the length of the body (not including the oral cone or carapace), one-fifth the length of the body including the oral cone but not the carapace and one-sixth of the length of the body including both the oral cone and the carapace. Taking this specimen alone gives a length of *ca* 9–11 mm for the Welsh hurdiid, although the more incomplete appendages in *Hurdia* specimens preserved in dorsal and lateral view indicate that frontal appendages of other specimens may have been shorter relative to body length (e.g. [28: fig. 3]). The comparison that gives the largest estimate for the body of the Welsh hurdiid comes from *Cambroraster*. A single specimen shows a well-preserved appendage adjacent to an isolated central carapace element [26: fig. 1g], and the length along the distal margin of this appendage is approximately one-fifth of the length from the anteriormost point of the carapace to the posteriormost point. The central carapace element in the holotype of *C. falcatus* [26: fig. 1a,b] extends over three-quarters of the total length of the animal. This ratio gives a conservative estimate that the frontal appendage is one-eighth of the total animal length. Extrapolating this for the Welsh hurdiid yields a body length of 15 mm, albeit based on numerous assumptions and approximations. Given the unusual ratio of frontal appendage size to body length in the eudemersal *Cambroraster* compared with other hurdiids, it is likely that the size of the Afon Gam radiodont was towards the lower end of the likely range suggested here (6–15 mm), and it is, therefore, likely that this animal represents the smallest known radiodont, although the significant uncertainties in these extrapolations should be acknowledged. Regardless, the size of the frontal appendage of the Welsh hurdiid is less than half that of the next smallest radiodont known, a 16 mm long juvenile *Lyrarapax* from the Chengjiang Biota with a well-preserved appendage *ca* 4–5 mm long (measured along the dorsal margin) [20]. The very small size of the Welsh hurdiid is consistent with the generally small size of other non-trilobite euarthropods from the Afon Gam Biota [49].

The status of the Welsh specimen as an adult or juvenile cannot be determined beyond doubt from only a single specimen, and indeed, very little is known about radiodont development. The few juveniles identified—the *Lyrarapax* mentioned above [20] and a small specimen of *A. symbrachiata*, also from the Chengjiang Biota [9: fig. 3], which measures *ca* 90 mm in body length (frontal appendages *ca* 20 mm)—show few morphological differences in their frontal appendages to adults of the same species, with no significant changes in the length of the terminal spine. A change in the orientation of auxiliary spines cannot be evaluated for *A. symbrachiata* or *L. trilobus* as this character is not preserved in the juvenile of the former radiodont, and is not known in the juvenile or adult of the latter [9,15,16,20]. The single row of small spines on the hypertrophied endite in *L. unguispinus* does not appear to be different in either the smallest (16 mm body length) specimen [20] or the largest (*ca* 80 mm body length) [15]. It is not known whether juvenile radiodonts were preceded by a larval stage, but from the current data, it would be expected that should the Afon Gam hurdiid specimen represent a juvenile, the adult would display a similar morphology. This consideration strongly implies that both the characters observed in this animal that are not known in other hurdiids—the orientation of the auxiliary spines and the length of the terminal spine relative to appendage length—would be present in adult specimens, regardless of whether the single specimen preserved is an adult or a juvenile.

5.2. Adaptability of Radiodonta

This description of a radiodont from the Afon Gam Biota, the first from Avalonia and the UK, adds to the substantial evidence supporting a wide geographical spread for this group in the early Palaeozoic. As the second Ordovician deposit from which a radiodont has been discovered, after the Fezouata Biota [32,33], this occurrence of a hurdiid radiodont on a new palaeocontinent provides a rare data point for understanding the post-Cambrian geographical range and diversity of this clade. Radiodonts are well known from Cambrian *Konservat-Lagerstätten*, on account of the relatively high preservation potential of their lightly sclerotized frontal appendages and oral cones, and their large size, while their ecological adaptability allowed them to exploit infaunal, epifaunal and planktonic food sources (e.g. [20,26–29,31,33,35,39]). However, this report of a centimetre-sized radiodont from an environment not rich in macroscopic, epifaunal food sources or other euarthropods shows a complementary way in which radiodonts were able to adapt to different environments, in this case to one in which the majority of other euarthropods appear to have been unable to thrive.

The Afon Gam Biota was probably a more hostile environment for radiodonts, and euarthropods in general, than the Cambrian BST *Konservat-Lagerstätten* from which they are best known, and the near-contemporaneous Fezouata Biota. This is demonstrated by the very different ecological balance in these BST faunas compared with the Ordovician Welsh deposit (e.g. [46,49,58]). The observed faunal composition within the Afon Gam Biota apparently left little for a large macropredator to consume, as the majority of preserved, motile epifaunal animals were biomineralized, in contrast with the wide variety of soft or lightly sclerotized motile epifaunal prey known from Cambrian BSTs and the Fezouata Biota. This is emphasized by the lack of large euarthropods known (so far) in the Afon Gam Biota [49], and by the presence of a wide variety of euarthropods of different sizes, including hurdiid radiodonts, in the Fezouata Biota [32,33]. The abundant worm fauna of the Afon Gam Biota, indicated largely by tubes and lined burrows [49,57], appears to have been dominantly infaunal. The question of whether the new radiodont described here shows adaptations to specific environmental differences between the Afon Gam Biota and other radiodont-bearing deposits should be considered in the light of the Ordovician ecological context. A recent detailed stratigraphic study of the early Cambrian Chengjiang biota demonstrated two distinct types of horizon: sponge-dominated background beds and euarthropod-dominated event beds, reflecting deep dysoxic and shallow oxic environments, respectively [82]; some other early Cambrian exceptionally preserved faunas from deep-water settings are also sponge-dominated [83]. However, the Afon Gam trilobite fauna closely resembles that of the shallow-water Sheinton Shales of Shropshire, and sedimentological data suggest that the Dol-cyn-Afon Formation was most likely not deposited in a deep-water setting [49].

Similarly, although some modern demosponges are able to thrive in very low-oxygen conditions (e.g. [84]), that may not be the case for other sponge groups, and there are many modern sponge-dominated communities that are not related to low oxygen levels. Indeed, the factors controlling sponge dominance are diverse; these faunas are typically associated with high nutrient levels (e.g. upwelling zones), but also other factors such as steeper slopes [85]. As sponge-dominated Ordovician assemblages also occur more widely in Wales [65,86], and the Afon Gam Biota includes a diverse range of taxa such as echinoderms

and tubiculous worms, and infauna, invoking low oxygenation to explain the ecology of the Afon Gam Biota does not seem justifiable; regional or wider ecological shifts must, therefore, be considered.

Strikingly, the largest radiodont ever discovered, the 2 m long hurdiid *A. benmoulai*, is from the near-contemporaneous Early Ordovician Fezouata Biota [32,33]. This Moroccan giant is two to three orders of magnitude larger than the Welsh hurdiid. In contrast with Cambrian BSTs, which are generally euarthropod-dominated and show remarkable consistency even at the genus level across multiple palaeocontinents over an approximately 25 Myr time span [46,63], Ordovician and younger *Konservat-Lagerstätten* exhibit marked disparities in their biotic compositions. Sponge-dominated sites, such as the Afon Gam Biota, are known from the Ordovician of Wales [63,65,86,87], and also from Cambrian and Ordovician strata of China [66,83], whereas Late Ordovician *Konservat-Lagerstätten* of Canada contain marginal-marine algal- or euarthropod-dominated assemblages [88,89], and the Silurian Kalana Formation preserves an exquisite algal fauna alongside crinoids and other non-euarthropod animals [90–93]. During the Ordovician biodiversification, within-community (α), between-community (β) and inter-provincial (γ) diversity all increased [94], resulting in greater differences between communities (including those preserved in *Konservat-Lagerstätten*) during the Ordovician than in the Cambrian. This pattern is clearly apparent when comparing the Cambrian and Ordovician sponge faunas [63]. In addition, at a global scale, the Ordovician biodiversification involved a pronounced shift towards suspension feeding and a reduction in mobile benthic predators (e.g. [94,95]). The rise of large nektonic predators such as orthocone nautiloids and eurypterids limited the role for radiodonts as apex predators during the Ordovician, and the convergent evolution of jaws in the Silurian increased the competition for this ecospace yet further [96,97]. The exploration of a vast range in body sizes within Ordovician radiodonts may reflect adaptations to the early stages of these global ecological changes.

For the specific case of the Afon Gam Biota, the small size of the hurdiid radiodont may reflect an adaptation to the small size and low abundance of epifaunal motile non-biomineralized prey in the environment.

6. Conclusion

The description of a miniature hurdiid from an Ordovician *Konservat-Lagerstätte* in Wales is the first report of a radiodont from palaeocontinent Avalonia and the modern-day UK. This animal has the smallest known frontal appendages of any member of Radiodonta. An extrapolation of its body size from this small frontal appendage suggests that this animal is the smallest hurdiid and probably the smallest radiodont ever discovered.

This paper is also the first report of a radiodont from an environment not dominated by euarthropods and highlights the adaptability of the group to a changing Ordovician world. There are greater differences between different Ordovician communities than their Cambrian counterparts, and available ecospace for large nektonic predators was restricted yet further by the emergence of other groups such as orthocone nautiloids. The small size of the Welsh hurdiid is interpreted as one adaptation towards the local ecological conditions of the sponge-dominated Dol-cyn-Afon Formation. Two alternative explanations, that the water depth or oxygenation at Afon Gam sites was significantly different to Cambrian *Konservat-Lagerstätten*, are rejected based on the co-occurring fauna.

Data accessibility. The specimen studied here is accessioned at Amgueddfa Cymru-National Museum Wales under accession NMW 2012.36G. No additional data were generated during the course of the study.

Authors' contributions. J.P.B. and L.A.M. performed the original fieldwork; J.P.B., L.M.E.M. and S.P. took the photographs; S.P. led analysis and interpretation of the fossil with intellectual input from all other authors; S.P. drafted the first version of the manuscript, all authors contributed intellectually critical content and revisions; all authors gave final approval for the final version and agree to be accountable for all aspects of the work in ensuring that questions related to the accuracy or integrity of any part of the work are appropriately investigated and resolved.

Competing interests. The authors declare no competing interests.

Funding. The specimen was collected through funding from the National Geographic Society's Committee for Research and Exploration (grant no. 9063-12) to J.P.B. S.P. acknowledges support from an Alexander Agassiz Postdoctoral Fellowship. J.P.B., L.M.E.M. and L.A.M. acknowledge support from Amgueddfa Cymru-National Museum Wales. Published by a grant from the Wetmore Colles fund.

Acknowledgements. We thank Chris Upton, Naomi Jordan and Neil Owen for assistance on fieldwork. We thank the Associate Editor Prof. Rachel Wood and two anonymous reviewers for their constructive comments which greatly improved the text, and R.D.C. Bicknell for comments on eurypterid appendages.

1. Conway Morris S. 1989 The persistence of Burgess Shale-type faunas: implications for the evolution of deeper-water faunas. *Earth Environ. Sci. Trans. R. Soc. Edinb.* **80**, 271–283. (doi:10.1017/S0263593300028716)
2. Gaines RR. 2014 Burgess Shale-type preservation and its distribution in space and time. *Paleontol. Soc. Pap.* **20**, 123–146. (doi:10.1017/S1089332600002837)
3. Muscente AD *et al.* 2017 Exceptionally preserved fossil assemblages through geologic time and space. *Gondwana Res.* **48**, 164–188. (doi:10.1016/j.gr.2017.04.020)
4. Daley AC, Antcliff JB, Drage HB, Pates S. 2018 Early fossil record of Euarthropoda and the Cambrian Explosion. *Proc. Natl Acad. Sci. USA* **115**, 5323–5331. (doi:10.1073/pnas.1719962115)
5. Briggs DEG. 1979 *Anomalocaris*, the largest known Cambrian arthropod. *Palaeontology* **22**, 631–664.
6. Briggs DEG, Mount JD. 1982 The occurrence of the giant arthropod *Anomalocaris* in the Lower Cambrian of southern California, and the overall distribution of the genus. *J. Paleontol.* **56**, 1112–1118.
7. Whittington HB, Briggs DEG. 1985 The largest Cambrian animal, *Anomalocaris*, Burgess Shale, British-Columbia. *Phil. Trans. R. Soc. Lond. B* **309**, 569–609. (doi:10.1098/rstb.1985.0096)
8. Lieberman BS. 2003 A new soft-bodied fauna: the Pioche Formation of Nevada. *J. Paleontol.* **77**, 674–690. (doi:10.1017/S002233600044413)
9. Chen JY, Ramsköld L, Zhou GQ. 1994 Evidence for monophyly and arthropod affinity of Cambrian giant predators. *Science* **264**, 1304–1308. (doi:10.1126/science.264.5163.1304)
10. Hou X-G, Bergström J, Ahlberg P. 1995 *Anomalocaris* and other large animals in the Lower Cambrian Chengjiang fauna of southwest China. *GFF* **117**, 163–183. (doi:10.1080/11035899509546213)
11. Daley AC, Edgecombe GD. 2014 Morphology of *Anomalocaris canadensis* from the Burgess Shale. *J. Paleontol.* **88**, 68–91. (doi:10.1666/13-067)
12. Pates S, Daley AC. 2019 The Kinzers Formation (Pennsylvania, USA): the most diverse assemblage of Cambrian Stage 4 radiodonts. *Geol. Mag.* **156**, 1233–1246. (doi:10.1017/S0016756818000547)
13. Pates S, Daley AC, Edgecombe GD, Cong P, Lieberman BS. 2019 Systematics, preservation and biogeography of radiodonts from the southern Great Basin, USA, during the upper Dyeran (Cambrian Series 2, Stage 4). *Pap. Palaeontol.* (doi:10.1002/spp2.1277)
14. Ortega-Hernández J. 2016 Making sense of 'lower' and 'upper' stem-group Euarthropoda, with comments on the strict use of the name Arthropoda von Siebold, 1848. *Biol. Rev.* **91**, 255–273. (doi:10.1111/brv.12168)
15. Cong P, Ma X, Hou X-G, Edgecombe GD, Strausfeld NJ. 2014 Brain structure resolves the segmental affinity of anomalocaridid appendages. *Nature* **513**, 538–542. (doi:10.1038/nature13486)
16. Cong P, Daley AC, Edgecombe GD, Hou X-G, Chen A. 2016 Morphology of the radiodontan *Lyrarapax* from the early Cambrian Chengjiang biota. *J. Paleontol.* **90**, 663–671. (doi:10.1017/jpa.2016.67)
17. Cong P, Daley AC, Edgecombe GD, Hou X-G. 2017 The functional head of the Cambrian radiodontan (stem-group Euarthropoda) *Amplectobelua symbrachiata*. *BMC Evol. Biol.* **17**, 208. (doi:10.1186/s12862-017-1049-1)
18. Cong P, Edgecombe GD, Daley AC, Guo J, Pates S, Hou X-G. 2018 New radiodonts with gnathobase-like structures from the Cambrian Chengjiang biota and implications for the systematics of Radiodonta. *Pap. Palaeontol.* **4**, 605–621. (doi:10.1002/spp2.1219)
19. Guo J, Pates S, Cong P, Daley AC, Edgecombe GD, Chen T, Hou X-G. 2019 A new radiodont (stem Euarthropoda) frontal appendage with a mosaic of characters from the Cambrian (Series 2 Stage 3) Chengjiang biota. *Pap. Palaeontol.* **5**, 99–110. (doi:10.1002/spp2.1231)
20. Liu J, Lerosey-Aubril R, Steiner M, Dunlop JA, Shu D, Paterson JR. 2018 Origin of raptorial feeding in juvenile euarthropods revealed by a Cambrian radiodontan. *Natl Sci. Rev.* **5**, 863–869. (doi:10.1093/nsr/nwy057)
21. Caron JB, Gaines RR, Mángano MG, Streng M, Daley AC. 2010 A new Burgess Shale-type assemblage from the 'thin' Stephen Formation of the southern Canadian Rockies. *Geology* **38**, 811–814. (doi:10.1130/G31080.1)
22. Pates S, Daley AC, Lieberman BS. 2018 Hurdiiid radiodontans from the middle Cambrian (Series 3) of Utah. *J. Paleontol.* **92**, 99–113. (doi:10.1017/jpa.2017.11)
23. Pates S, Daley AC, Ortega-Hernández J. 2017 *Aysheaia prolata* from the Wheeler Formation (Cambrian, Drumian) is a frontal appendage of the radiodontan *Stanleycaris*. *Acta Palaeontol. Pol.* **62**, 619–625. (doi:10.4202/app.00361.2017)
24. Pates S, Daley AC, Butterfield NJ. 2019 First report of paired ventral endites in a hurdiid radiodont. *Zool. Lett.* **5**, 18. (doi:10.1186/s40851-019-0132-4)
25. Pates S, Daley AC. 2017 *Caryosyntrips*: a radiodontan from the Cambrian of Spain, USA and Canada. *Pap. Palaeontol.* **3**, 461–470. (doi:10.1002/spp2.1084)
26. Moysiuk J, Caron JB. 2019 A new hurdiid radiodont from the Burgess Shale evinces the exploitation of Cambrian infaunal food sources. *Proc. R. Soc. B* **286**, 20191079. (doi:10.1098/rspb.2019.1079)
27. Daley AC, Budd GE, Caron JB, Edgecombe GD, Collins D. 2009 The Burgess Shale anomalocaridid *Hurdia* and its significance for early euarthropod evolution. *Science* **323**, 1597–1600. (doi:10.1126/science.1169514)
28. Daley AC, Budd GE, Caron JB. 2013 Morphology and systematics of the anomalocaridid arthropod *Hurdia* from the Middle Cambrian of British Columbia and Utah. *J. Syst. Paleontol.* **11**, 743–787. (doi:10.1080/14772019.2012.732723)
29. Daley AC, Budd GE. 2010 New anomalocaridid appendages from the Burgess Shale, Canada. *Palaeontology* **53**, 721–738. (doi:10.1111/j.1475-4983.2010.00955.x)
30. Daley AC, Legg DA. 2015 A morphological and taxonomic appraisal of the oldest anomalocaridid from the lower Cambrian of Poland. *Geol. Mag.* **152**, 949–955. (doi:10.1017/S0016756815000412)
31. Vinther J, Stein M, Longrich NR, Harper DA. 2014 A suspension-feeding anomalocarid from the Early Cambrian. *Nature* **507**, 496–499. (doi:10.1038/nature13010)
32. Van Roy P, Briggs DEG. 2011 A giant Ordovician anomalocaridid. *Nature* **473**, 510–513. (doi:10.1038/nature09920)
33. Van Roy P, Daley AC, Briggs DEG. 2015 Anomalocaridid trunk limb homology revealed by a giant filter-feeder with paired flaps. *Nature* **522**, 77–80. (doi:10.1038/nature14256)
34. McHenry B, Yates A. 1993 First report of the enigmatic metazoan *Anomalocaris* from the Southern Hemisphere and a trilobite with preserved appendages from the Early Cambrian of Kangaroo Island, South Australia. *Rec. South Aust. Mus.* **26**, 77–86.
35. Daley AC, Paterson JR, Edgecombe GD, García-Bellido DC, Jago JB. 2013 New anatomical information on *Anomalocaris* from the Cambrian Emu Bay Shale of South Australia and a reassessment of its inferred predatory habits. *Palaeontology* **56**, 971–990. (doi:10.1111/pala.12029)
36. Nedin C. 1999 *Anomalocaris* predation on nonmineralized and mineralized trilobites. *Geology* **27**, 987–990. (doi:10.1130/0091-7613(1999)027<0987:APONAM>2.3.CO;2)
37. Briggs DEG, Robison RA. 1984 Exceptionally preserved nontrilobite arthropods and *Anomalocaris* from the Middle Cambrian of Utah. *Univ. Kansas Paleontol. Contrib.* **111**, 1–23.
38. Conway Morris S, Robison RA. 1988 More soft-bodied animals and algae from the Middle Cambrian of Utah and British Columbia. *Univ. Kansas Paleontol. Contrib.* **122**, 1–48.
39. Lerosey-Aubril R, Pates S. 2018 New suspension-feeding radiodont suggests evolution of microplanktivory in Cambrian macronekton. *Nat. Commun.* **9**, 1–9. (doi:10.1038/s41467-018-06229-7)
40. Hou X-G, Bergström J. 2003 The Chengjiang fauna—the oldest preserved animal community. *Paleontol. Res.* **7**, 55–70. (doi:10.2517/prpsj.7.55)
41. Caron J-B, Jackson DA. 2008 Paleoecology of the greater phyllopod bed community, Burgess Shale. *Palaeogeogr. Palaeoclimatol. Palaeoecol.* **258**, 222–256. (doi:10.1016/j.palaeo.2007.05.023)
42. Paterson JR, García-Bellido DC, Jago JB, Gehling JG, Lee MS, Edgecombe GD. 2016 The Emu Bay Shale Konservat-Lagerstätte: a view of Cambrian life from East Gondwana. *J. Geol. Soc.* **173**, 1–11. (doi:10.1144/jgs2015-083)

43. Lerosee-Aubril R, Gaines RR, Hegna TA, Ortega-Hernández J, Van Roy P, Kier C, Bonino E. 2018 The Weeks Formation Konservat-Lagerstätte and the evolutionary transition of Cambrian marine life. *J. Geol. Soc.* **175**, 705–715. (doi:10.1144/jgs2018-042)
44. Kimmig J, Strotz LC, Kimmig SR, Egenhoff SO, Lieberman BS. 2019 The Spence Shale Lagerstätte: an important window into Cambrian biodiversity. *J. Geol. Soc.* **176**, 609–619. (doi:10.1144/jgs2018-195)
45. Fu D *et al.* 2019 The Qingjiang biota—a Burgess Shale-type fossil lagerstätte from the early Cambrian of South China. *Science* **363**, 1338–1342. (doi:10.1126/science.aau8800)
46. Holmes JD, García-Bellido DC, Lee MS. 2018 Comparisons between Cambrian Lagerstätten assemblages using multivariate, parsimony and Bayesian methods. *Gondwana Res.* **55**, 30–41. (doi:10.1016/j.jgr.2017.10.007)
47. Zhao F, Hu S, Caron J-B, Zhu M, Yin Z, Lu M. 2012 Spatial variation in the diversity and composition of the Lower Cambrian (Series 2, Stage 3) Chengjiang biota, Southwest China. *Palaeogeogr. Palaeoclimatol. Palaeoecol.* **346**, 54–65. (doi:10.1016/j.palaeo.2012.05.021)
48. Nanglu K, Caron J-B, Gaines RR. 2020 The Burgess Shale paleocommunity with new insights from Marble Canyon, British Columbia. *Paleobiology* **46**, 58–81. (doi:10.1017/pab.2019.42)
49. Botting JP, Muir LA, Jordan N, Upton C. 2015 An Ordovician variation on Burgess Shale-type biotas. *Sci. Rep.* **5**, 9947. (doi:10.1038/srep09947)
50. Müller RD *et al.* 2018 GPlates: building a virtual Earth through deep time. *Geochem. Geophys. Geosyst.* **19**, 2243–2261. (doi:10.1029/2018GC007584)
51. Cocks LR, Fortey RA. 2009 Avalonia: a long-lived terrane in the Lower Palaeozoic? *Geol. Soc. Lond. Spec. Publ.* **325**, 141–155. (doi:10.1144/SP325.7)
52. Mac Niocaill C, Van der Pluijm BA, Van der Voo R. 1997 Ordovician paleogeography and the evolution of the Iapetus ocean. *Geology* **25**, 159–162. (doi:10.1130/0091-7613(1997)025<0159:OPATEO>2.3.CO;2)
53. Scotese CR, Wright N. 2018 PALEOMAP paleodigital elevation models (PaleoDEMs) for the Phanerozoic. See <https://www.earthbyte.org/paleodem-resource-scotese-and-wright-2018>.
54. Torsvik TH, Cocks LR. 2013 Gondwana from top to base in space and time. *Gondwana Res.* **24**, 999–1030. (doi:10.1016/j.jgr.2013.06.012)
55. Cocks LR, Torsvik TH. 2002 Earth geography from 500 to 400 million years ago: a faunal and palaeomagnetic review. *J. Geol. Soc.* **159**, 631–644. (doi:10.1144/0016-764901-118)
56. Daley AC, Drage HB. 2016 The fossil record of ecdysis, and trends in the moulting behaviour of trilobites. *Arthropod. Struct. Dev.* **45**, 71–96. (doi:10.1016/j.asd.2015.09.004)
57. Muir LA, Botting JP, Lefebvre B, Upton C, Zhang YD. 2019 Agglutinated tubes as a feature of Early Ordovician ecosystems. *Palaeoworld* **28**, 96–109. (doi:10.1016/j.palwor.2019.01.004)
58. Van Roy P, Briggs DEG, Gaines RR. 2015 The Fezouata fossils of Morocco; an extraordinary record of marine life in the Early Ordovician. *J. Geol. Soc.* **172**, 541–549. (doi:10.1144/jgs2015-017)
59. Martin EL *et al.* 2016 The Lower Ordovician Fezouata Konservat-Lagerstätte from Morocco: age, environment and evolutionary perspectives. *Gondwana Res.* **34**, 274–283. (doi:10.1016/j.jgr.2015.03.009)
60. Botting JP. 2016 Diversity and ecology of sponges in the Early Ordovician Fezouata Biota, Morocco. *Palaeogeogr. Palaeoclimatol. Palaeoecol.* **460**, 75–86. (doi:10.1016/j.palaeo.2016.05.018)
61. Lefebvre B, Lerosee-Aubril R, Servais T, Van Roy P. 2016 The Fezouata Biota: an exceptional window on the Cambro-Ordovician faunal transition. *Palaeogeogr. Palaeoclimatol. Palaeoecol.* **460**, 1–6. (doi:10.1016/j.palaeo.2016.06.041)
62. Hou X-G, Siveter DJ, Siveter DJ, Aldridge RJ, Cong P, Gabbott SE, Ma X, Purnell MA, Williams M. 2017 *The Cambrian fossils of Chengjiang, China: the flowering of early animal life*. Oxford, UK: John Wiley & Sons.
63. Botting JP, Muir LA. 2019 Dispersal and endemic diversification: differences in non-lithistid spiculate sponge faunas between the Cambrian Explosion and the GOBE. *Palaeoworld* **28**, 24–36. (doi:10.1016/j.palwor.2018.03.002)
64. Saleh F, Candela Y, Harper DA, Polechová M, Lefebvre B, Pittet B. 2018 Storm-induced community dynamics in the Fezouata Biota (Lower Ordovician, Morocco). *PALAIOS* **33**, 535–541. (doi:10.2110/palo.2018.055)
65. Botting JP, Muir LA, Sutton MD, Barnie T. 2011 Welsh gold: a new exceptionally preserved pyritized Ordovician biota. *Geology* **39**, 879–882. (doi:10.1130/G32143.1)
66. Botting JP, Muir LA, Zhang Y, Ma X, Ma J, Wang L, Zhang J, Song Y, Fang X. 2017 Flourishing sponge-based ecosystems after the end-Ordovician mass extinction. *Curr. Biol.* **27**, 556–562. (doi:10.1016/j.cub.2016.12.061)
67. Gerhardt AM, Gill BC. 2016 Elucidating the relationship between the later Cambrian end-Marjuman extinctions and SPICE Event. *Palaeogeogr. Palaeoclimatol. Palaeoecol.* **461**, 362–373. (doi:10.1016/j.palaeo.2016.08.031)
68. Muscente AD, Prabhu A, Zhong H, Elish A, Meyer MB, Fox P, Hazen RM, Knoll AH. 2018 Quantifying ecological impacts of mass extinctions with network analysis of fossil communities. *Proc. Natl Acad. Sci. USA* **115**, 5217–5222. (doi:10.1073/pnas.1719976115)
69. Tollerton VP. 1989 Morphology, taxonomy, and classification of the order Eurypterida Burmeister, 1843. *J. Paleontol.* **63**, 642–657. (doi:10.1017/S0022336000041275)
70. Waterston CD, Oelofsen BW, Oosthuizen RD. 1985 *Cyrtoctenus wittebergensis* sp. nov. (Chelicerata: Eurypterida), a large sweep-feeder from the Carboniferous of South Africa. *Earth Environ. Sci. Trans. R. Soc. Edinb.* **76**, 339–358. (doi:10.1017/S0263593300010555)
71. Gámez Vintaned JA, Linán E, Zhuravlev AY. 2011 A new early Cambrian lobopod-bearing animal (Murero, Spain) and the problem of the ecdysozoan early diversification. In *Evolutionary biology—concepts, biodiversity, macroevolution and genome evolution* (ed. P. Pontarotti), pp. 193–219. Berlin, Germany: Springer.
72. Gámez Vintaned JA, Zhuravlev AY. 2018 Comment on ‘*Aysheaia prolata* from the Utah Wheeler Formation (Drumian, Cambrian) is a frontal appendage of the radiodontan *Stanleycaris*’ by Stephen Pates, Allison C. Daley, and Javier Ortega-Hernández. *Acta Palaeontol. Pol.* **63**, 103–104.
73. Pates S, Daley AC, Ortega-Hernández J. 2018 Reply to Comment on ‘*Aysheaia prolata* from the Utah Wheeler Formation (Drumian, Cambrian) is a frontal appendage of the radiodontan *Stanleycaris*’ with the formal description of *Stanleycaris*. *Acta Palaeontol. Pol.* **63**, 105–110. (doi:10.4202/app.00443.2017)
74. Lamsdell JC, Briggs DE, Liu HP, Witzke BJ, McKay RM. 2015 The oldest described eurypterid: a giant Middle Ordovician (Darrivillan) megalograptid from the Winneshiek Lagerstätte of Iowa. *BMC Evol. Biol.* **15**, 169. (doi:10.1186/s12862-015-0443-9)
75. Braddy SJ, Aldridge RJ, Theron JN. 1995 A new eurypterid from the Late Ordovician Table Mountain Group, South Africa. *Palaeontology* **38**, 563–582.
76. Stott CA, Tettie OE, Braddy SJ, Nowlan GS, Glasser PM, Devereux MG. 2005 A new eurypterid (chelicerata) from the Upper Ordovician of Manitoulin Island, Ontario, Canada. *J. Paleontol.* **79**, 1166–1174. (doi:10.1666/0022-3360(2005)079[1166:ANEFT]2.0.CO;2)
77. Lamsdell JC, Braddy SJ. 2010 Cope’s Rule and Romer’s theory: patterns of diversity and gigantism in eurypterids and Palaeozoic vertebrates. *Biol. Lett.* **6**, 265–269. (doi:10.1098/rsbl.2009.0700)
78. Lamsdell JC, Hoşgör İ, Selden PA. 2013 A new Ordovician eurypterid (Arthropoda: Chelicerata) from southeast Turkey: evidence for a cryptic Ordovician record of Eurypterida. *Gondwana Res.* **23**, 354–366. (doi:10.1016/j.jgr.2012.04.006)
79. Størmer L, Waterston CD. 1968 *Cyrtoctenus* gen. nov., a large late Palaeozoic arthropod with pectinate appendages. *Earth Environ. Sci. Trans. R. Soc. Edinb.* **68**, 63–104. (doi:10.1017/S0080456800014563)
80. Lamsdell JC, Selden PA. 2017 From success to persistence: identifying an evolutionary regime shift in the diverse Paleozoic aquatic arthropod group Eurypterida, driven by the Devonian biotic crisis. *Evolution* **71**, 95–110. (doi:10.1111/evo.13106)
81. Jeram AJ, Selden PA. 1994 Eurypterids from the Viséan of East Kirkton, West Lothian, Scotland. *Earth Environ. Sci. Trans. R. Soc. Edinb.* **84**, 301–308. (doi:10.1017/S0263593300006118)
82. Qi C, Li C, Gabbott SE, Ma X, Xie L, Deng W, Jin C, Hou XG. 2018 Influence of redox conditions on animal distribution and soft-bodied fossil preservation of the Lower Cambrian Chengjiang Biota. *Palaeogeogr. Palaeoclimatol. Palaeoecol.* **507**, 180–187. (doi:10.1016/j.palaeo.2018.07.010)
83. Xiao S, Hu J, Yuan X, Parsley RL, Cao R. 2005 Articulated sponges from the Lower Cambrian Hetang Formation in southern Anhui, South

- China: their age and implications for the early evolution of sponges. *Palaeogeogr. Palaeoclimatol. Palaeoecol.* **220**, 89–117. (doi:10.1016/j.palaeo.2002.02.001)
84. Mills DB, Ward LM, Jones C, Sweeten B, Forth M, Treusch AH, Canfield DE. 2014 Oxygen requirements of the earliest animals. *Proc. Natl Acad. Sci. USA* **111**, 4168–4172. (doi:10.1073/pnas.1400547111)
85. Maldonado M, Young CM. 1996 Bathymetric patterns of sponge distribution on the Bahamian slope. *Deep Sea Res. Part I* **43**, 897–915. (doi:10.1016/0967-0637(96)00042-8)
86. Muir LA, Botting JP. 2015 An outline of the distribution and diversity of Porifera in the Ordovician Builth Inlier (Wales, UK). *Palaeoworld* **24**, 176–190. (doi:10.1016/j.palwor.2014.11.003)
87. Botting JP, Muir LA. 2012 First post-Cambrian records of the reticulosan sponges *Valospongia* and *Hintzespongia* from the late Tremadocian of North Wales. *Acta Palaeontol. Pol.* **59**, 241–252.
88. Young GA, Rudkin DM, Dobrzanski EP, Robson SP, Nowlan GS. 2007 Exceptionally preserved late Ordovician biotas from Manitoba, Canada. *Geology* **35**, 883–886. (doi:10.1130/G23947A.1)
89. Young G, Rudkin D, Dobrzanski E, Robson S, Cuggy M, Demski M, Thompson D. 2012 Great Canadian Lagerstätten 3. Late Ordovician Konservat-Lagerstätten in Manitoba. *Geosci. Canada* **39**, 201–213.
90. Tinn O, Meidla T, Ainsaar L, Pani T. 2009 Thallophtic algal flora from a new Silurian Lagerstätte. *Est. J. Earth Sci.* **58**, 38–42. (doi:10.3176/earth.2009.1.04)
91. Tinn O, Mastik V, Ainsaar L, Meidla T. 2015 *Kalania pusilla*, an exceptionally preserved non-calcified alga from the lower Silurian (Aeronian. Llandovery) of Estonia. *Palaeoworld* **24**, 207–214. (doi:10.1016/j.palwor.2014.12.001)
92. Mastik V, Tinn O. 2015 New dasycladalean algal species from the Kalana Lagerstätte (Silurian, Estonia). *J. Paleontol.* **89**, 262–268. (doi:10.1017/jpa.2014.23)
93. Ausich WI, Wilson MA, Tinn O. 2020 Kalana Lagerstätte crinoids: Early Silurian (Llandovery) of central Estonia. *J. Paleontol.* **94**, 131–144. (doi:10.1017/jpa.2019.27)
94. Servais T, Owen AW, Harper DA, Kröger B, Munnecke A. 2010 The great Ordovician biodiversification event (GOBE): the palaeoecological dimension. *Palaeogeogr. Palaeoclimatol. Palaeoecol.* **294**, 99–119. (doi:10.1016/j.palaeo.2010.05.031)
95. Servais T *et al.* 2016 The onset of the ‘Ordovician Plankton Revolution’ in the late Cambrian. *Palaeogeogr. Palaeoclimatol. Palaeoecol.* **458**, 12–28. (doi:10.1016/j.palaeo.2015.11.003)
96. Klug C, Frey L, Pohle A, De Baets K, Korn D. 2017 Palaeozoic evolution of animal mouthparts. *Bull. Geosci.* **92**, 439–442. (doi:10.3140/bull.geosci.1648)
97. Kröger B, Servais T, Zhang Y. 2009 The origin and initial rise of pelagic cephalopods in the Ordovician. *PLoS ONE* **4**, e7262. (doi:10.1371/journal.pone.0007262)